Indium clustering in *a*-plane InGaN quantum wells as evidenced by atom probe tomography

Fengzai Tang[1], Tongtong Zhu[1], Fabrice Oehler[1], Wai Yuen Fu[1], James T. Griffiths[1], Fabien C. -P. Massabuau[1], Menno J. Kappers[1], Tomas L. Martin[2], Paul A. J. Bagot[2], Michael P. Moody[2,a)] and Rachel A. Oliver[1,b)]

[1] *Department of Materials Science and Metallurgy, University of Cambridge, 27 Charles Babbage Road, Cambridge, CB3 0FS, United Kingdom*

[2] *Departments of Materials, University of Oxford, Parks Road, Oxford, OX1 3PH, United Kingdom*

Atom probe tomography (APT) has been used to characterize the distribution of In atoms within non-polar *a*-plane InGaN quantum wells (QWs) grown on a GaN pseudo-substrate produced using epitaxial lateral overgrowth. Application of the focused ion beam microscope enabled APT needles to be prepared from the low defect density regions of the grown sample. A complementary analysis was also undertaken on QWs having comparable In contents grown on polar *c*-plane sample pseudo-substrates. Both frequency distribution and modified nearest neighbor analyses indicate a statistically non-randomized In distribution in the *a*-plane QWs, but a random distribution in the *c*-plane QWs. This work not only provides insights into the structure of non-polar *a*-plane QWs, but also shows that APT is capable of detecting as-grown nanoscale clustering in InGaN and thus validates the reliability of earlier APT analyses of the In distribution in *c*-plane InGaN QWs which show no such clustering.

Key words: InGaN quantum wells; In clusters; Atom probe tomography

InGaN quantum wells (QWs) form the active layer of high efficiency blue and green light emitting diodes (LEDs).[1] Such devices are commonly grown on *c*-plane GaN grown heteroepitaxially on sapphire, silicon carbide or silicon. In this polar orientation, the InGaN QWs suffer from large internal electric fields, which may degrade the radiative recombination efficiency.[2] Hence, alternative non- and semi-polar planes are being explored, aiming to improve light emission efficiency by eliminating or reducing the internal electric fields along the growth direction.[3]

One surprising feature of InGaN QWs is that their light emission appears to be robust to the presence of threading dislocations with densities of 10^8 cm^{-2} or above,[4] despite the fact that evidence from cathodoluminescence suggests that these dislocations act as non-radiative recombination centers.[5] The efficient light emission from InGaN QWs has been attributed to carrier localization[6] preventing carrier diffusion to dislocation cores. Non-random clusters of In atoms were once thought to be the main localization center in *c*-plane $In_xGa_{1-x}N$ QWs (for x of around 0.2), a contention which has provoked an on-going debate.[7-13] Evidence for nanometer-scale In fluctuations was initially found using high resolution transmission electron microscopy (HRTEM).[11] However, studies by Smeeton *et al.*[12] suggested that InGaN

a) Electronic mail: michael.moody@materials.ox.ac.uk.

b) Electronic mail: rao28@cam.ac.uk.

QWs were sensitive to the high energy electron beam in TEM which could induce the formation of highly-strained regions which were then interpreted as In-rich clusters. These studies cast significant doubt on the identification of In clusters by HRTEM.

Atom probe tomography (APT) has the capacity to provide three dimensional (3D) chemical composition maps with near atomic resolution without the potentially detrimental electron-beam exposure inherent in TEM analysis. After the pioneering work by Galtrey et al.,[8] APT has been increasingly utilized to study In distributions in QWs grown on *c*-plane,[8,14] *m*-plane[15] and semi-polar[16] GaN by both metal organic vapor phase epitaxy (MOVPE) and molecular beam epitaxy (MBE). In these studies, the distribution of In atoms was ubiquitously found to be statistically random using frequency distribution (FD) analysis. These studies are increasingly held to demonstrate that In-clustering is not necessary for the efficient emission of light from InGaN. However, in the absence of any APT data indicating In-clustering, it may raise questions about the ability of APT to actually detect such clusters. Bennett *et al.*[17] used APT to study InGaN QWs exposed to an electron beam in the TEM and detected non-random clustering, but nonetheless, the effectiveness of the different characterization techniques for indium distribution analysis in as-grown material continues to be debated.

One challenge in the FD analysis approach to the APT data is the through-thickness variation[18] of the In content of the QW structures. Even if within the lateral plane In atoms are arranged randomly, such a systematic change in composition through the depth of the QW can result in a false positive when testing for non-randomness. Hence, this growth feature generally limits FD analysis to relatively thin sub-volumes of a QW in which this effect is minimized.[14,16] In addition, FD analysis is inherently influenced by sample size complicating direct comparison between different analyses.[19] In this work, a modified Nearest Neighbor (NN[20]) analysis has also been developed to better interpret the APT data. As is the case for FD, a conventional NN analysis of the In distribution would be biased by a systematic compositional variation through the depth of the QW. In the modified NN approach developed here, this effect is negated by projecting all of the atoms of a single QW onto a single plane, effectively compressing the reconstructed QW image in the depth direction. The NN analysis is then applied to characterize the distribution of neighboring lateral distances between neighboring In atoms in this plane. Effectively, the analysis identifies clustering within the lateral plane of the QW.

Both types of analysis reveal non-random In clustering in the *a*-plane QWs, whilst a *c*-plane sample with comparable In content shows no clustering when subjected to either form of analysis. Hence the work we present here verifies both the ability of APT to detect non-random clustering and the absence of such clustering in our *c*-plane samples.

The *a*-plane sample was grown on *r*-plane $\{1\bar{1}02\}$ sapphire using MOVPE in a Thomas Swan 6×2 inch close-coupled showerhead reactor. Trimethylgallium, trimethylindium and ammonia were used as precursors.

In order to reduce the defect density in the pseudo-substrate, an epitaxial lateral overgrowth (ELOG) technique (which we have described in detail elsewhere[21]) was used resulting in dislocation densities of less than 10^6 cm^{-2} in + *c* wing, ~ 9 × 10^8 cm^{-2} in - *c* wing and ~ 10^{10} cm^{-2} in window regions, and basal-plane stacking fault (BSF) densities of ~ 10^4 cm^{-1} in + *c* wing, and about 10^5 cm^{-1} for both - *c* wing and window areas. A five-period InGaN/GaN QW structure was grown on the ELOG template using a "quasi-two temperature method"[22] with an InGaN growth temperature of 695°C. X-ray diffraction (XRD) analysis was performed on a Philips/Panalytical PW3050/65 X'Pert PRO high resolution horizontal diffractometer using the method modified from Vickers *et al.*.[23] It showed an In fraction (x) of 0.15 ± 0.02 in $In_xGa_{1-x}N$, and QW and barrier thicknesses of 4 ± 0.2 nm and 7 ± 0.2 nm respectively. The thickness measurement was also consistent with TEM analysis. The *c*-plane sample did not employ an ELOG pseudo-substrate, and had a uniform threading dislocation density of ~ 5 × 10^8 cm^{-2}.[24] Ten *c*-plane InGaN/GaN QWs were grown using a quasi-two temperature method,[22] but with a higher InGaN growth temperature of 747°C, in order to achieve an indium fraction of 0.16 ± 0.01. In this case, XRD and TEM revealed QW and barrier thicknesses of 2.4 ± 0.1 nm and 7.3 ± 0.1 nm respectively.

Photoluminescence (PL) from the *a*- and *c*-plane samples was measured using an Accent RPM 2000 at room temperature, using a 266 nm Q-switched laser as an excitation source with an estimated average power density of 1MW/cm^2. In order to identify + *c* wing areas, the *a*-plane sample was examined using cathodoluminescence in the scanning electron microscope (SEM-CL): A Philips XL30. SEM fitted with a Gatan MonoCL4 system was employed.[25] The SEM was operated at 5 kV and the sample stage was cooled to ~ 90 K using liquid nitrogen. Site-specific samples from the identified + *c* wing areas were then prepared for APT analysis using a focused ion beam microscope (FIB: FEI Helios NanoLab™). The samples were mounted on a standard Si coupon. To minimize FIB-induced damage we employed sample surfaces pre-coated with a thin Pt layer, an electron-beam deposited Pt strap and a 'clean-up' procedure with the FIB voltage down to 1 kV. Details of the sample preparation process are given in reference.[26]

APT experiments were conducted in pulsed laser mode using a Cameca LEAP 3000X HR, where the base temperature of sample was set at ~ 30 K. Laser pulse energies of 0.004 nJ and 0.04 nJ were used on different *a*-plane APT tips, but with a constant detection rate of 0.005 atoms per pulse. Discussions in this paper are thus based on analysis of these two APT samples, but both yield similar results. The APT reconstruction was carried out using the IVAS™ software package (CAMECA Version 3.6.6) using the thicknesses of the InGaN/GaN layers measured by XRD and TEM and also the geometry of the tip as measured by SEM.

The SEM-CL analysis of the *a*-plane sample is depicted in Figs. 1(a) and (b), which show a panchromatic CL image and a CL spectrum from the corresponding area respectively. To identify the regions of + *c* wing (low defect density), - *c* wing and window, monochromatic CL images (not shown) were also recorded at 358 nm (GaN near band edge emission) and 362.5 nm (BSF emission).[25] The regions thus identified are labeled in Fig. 1(a). The large arrow indicates the position of the center of a wedge (~ 18 (l) × 2 (w) µm)

which was then extracted by FIB and from which APT samples were prepared. The peak of the CL emission in Fig. 1(b) is at about 475 nm, comparable to the room temperature PL measurement which showed emission at ~ 480 nm. The *c*-plane sample showed room temperature PL emission at ~ 440 nm. This is a surprising observation, given the similar compositions of the two samples, since we would expect the *a*-plane emission to be at a much shorter wavelength than the *c*-plane due to the absence of the internal electric field along the *a*-axis in the non-polar QWs.[2]

Figure 1(c) depicts a reconstruction of the 3D APT data from the *a*-plane sample following analysis at 0.004 nJ, showing the five InGaN QWs. For clarity, this figure shows 80% of the recorded In atoms and 10% of the Ga atoms, and the volume of the region shown is about 45 × 45 × 65 nm. The corresponding 1D concentration profile (Fig. 1(d)) shows that the In-fraction of the first QW is higher than that of the subsequent QWs and that the profile of the QW composition is not rectangular. Analysis at other laser energies gave rise to comparable In profiles, with no systematic variation in In content observed as a function of laser energy. Hereafter, we will focus on the In distributions in the first 3 QWs, closest to the substrate which were all analyzed at the same laser energy.

In the analysis of the APT data for both the *a*- and *c*-plane samples, for each QW we will define the lower and upper interfaces between the QW and the GaN barrier as that closest to and furthest from the substrate respectively. First, In concentration profiles through the depth of each QW were computed based on the lower interfaces using a proximity histogram (proxigram) approach. The maximum In content in each QW was determined from these profiles. As a typical example, Fig. 2 presents 2D projections of the extracted 2nd QWs of *a*- and *c*-plane samples using interfaces at the half maximum In contents, i.e., an In fraction of 0.075 for *a*-plane (Fig. 2(a)) and of 0.082 for *c*-plane (Fig. 2(b)). This *c*-plane QW was analyzed at 0.008 nJ. From a visual examination, some 'blotchy' areas associated with locally increased In atoms can be seen in the *a*-plane QW in Fig. 2(a), some of which are arrowed, whereas the *c*-plane QW does not appear to contain such features (Fig. 2(b)). It should be noted that the extracted *a*-plane QW in Fig. 2(a) has more In atoms than that c-plane (Fig. 2(b)), although the same processing criteria are employed. This is because the *a*-plane QW has a larger thickness than the *c*-plane. This effect is also seen in the larger frequency numbers in the FD and modified NN analyses.

Statistical assessment of the In distribution in the first 3 QWs in Fig. 1(c) was carried out using FD analysis and modified NN analysis. For the FD analysis, the sub-volume of each QW to be analyzed was isolated using the upper and lower isosurfaces defined by half the maximum In fraction. Only In and Ga atoms were included in the analysis. The analysis was performed iteratively with bin sizes that ranged from 25 to 200 atoms with a step size of 25 atoms, equivalent to analyzing volumes with linear dimension from about 1.2 to 2.4 nm.[16] For the modified NN analysis, a QW was first extracted from an APT reconstruction using a rectangular region-of-interest aligned parallel to the in-plane well. This was then projected onto a single plane approximately perpendicular to the growth direction. The distance distribution of each In atom and its

k^{th} nearest neighbor (kNN) In atom was calculated. To interpret these results a randomized comparator was created for each QW by randomly swapping chemical identities of all atoms within the projected data set, i.e. a complementary data set in which it is known that no statistically significant chemical-spatial correlation exist. The NN analysis was then repeated for this randomized comparator.

FD analysis of the data in Fig. 2 is shown in Fig. 3 for the case with a bin size of 75 atoms, as a typical example. Fig. 3(a) plots the experimentally observed In distribution (histogram) compared to the binomial distribution (blue curve) that would be theoretically observed for a random arrangement of QW In atoms within the *a*-plane sample. Fig. 3(b) reveals significant differences between the observed data and the model distribution. A similar analysis of the 2nd QW of *c*-plane sample is presented in Figs. 3(c) and (d), and suggests better agreement between model and data. In these figures cases with expected frequency number much less than 5 were combined into one frequency bin, as recommended in reference.[19] In order to quantitatively evaluate any deviation of the observed data from the random distributions, a χ^2 analysis was used, yielding a p-value less than 0.001 for the *a*-plane case (Fig. 3(b)) but a p-value 0.78 for *c*-plane case (Fig. 3(d)). Using a standard significance level of 5%,[19] the null hypothesis, i.e., a random In distribution, should be rejected for the case of *a*-plane, but accepted for the case of *c*-plane. Consistent results were obtained on all bin sizes studied, where in the vast majority of cases for the *a*-plane QW the p-value is < 0.001. Thus, the analysis indicates that In atoms are statistically non-randomly distributed in the *a*-plane QW, but randomly dispersed in the *c*-plane sample. Examination of the 1st and 3rd QWs of the *a*-plane and *c*-plane samples yields the same conclusion.

Figure 4 depicts the modified 25NN analysis from the 2nd QWs of both the *a*- and *c*-plane samples. For the *a*-plane QW, the observed distance distribution significantly deviates from its random comparator as illustrated in Fig. 4(a). In contrast, a close match between observed and expected distributions can be found in the *c*-plane sample (Fig. 4(b)), where the slight difference is likely due to statistical fluctuation and/or imperfections in the APT reconstruction. The 25NN analysis on the first and third QW in the *a*-plane sample yielded similar results. This indicates strong statistical evidence for clustering of In atoms in the *a*-plane sample, in agreement with the FD analysis in Fig. 3. It should be noted that although the 10NN and 25NN analyses on the 2nd *a*-plane QW show similar results, it is difficult to discriminate deviations at the low order kNN ($k < 5$) analysis, such as 1NN. This is due to the fact that the In content in the QW is relatively high, and thus the average distance between two very near neighbor In atoms in QW is close to that in the random case.

In summary, the In distribution has been studied in detail for the first 3 InGaN QWs taken from low defect density + *c* wing areas on an *a*-plane ELOG wafer grown by MOVPE. Both FD and modified NN analyses indicate that In atoms were statistically non-randomly distributed, i.e., clustered, in contrast to the case of *c*-plane. It should be noted that this difference between the *a*- and *c*-plane samples may be due either to the different kinetics and thermodynamics of growth on the different crystal planes, or to the different

thicknesses of the *a*- and *c*-plane QWs examined here, or to a combination of the two. Whilst this issue deserves further investigation, it does not invalidate a key conclusion which may be drawn: APT *is* capable of detecting as-grown nanoscale In-clusters, and thus *c*-plane data in which such clusters are *not* detected does indeed show that bright light emission is possible from such samples without In-clustering. Furthermore, we note again the unexpectedly long PL emission wavelength from the *a*-plane sample. The presence of clustering on a length scale of the order of a few nanometers on the *a*-plane (which *will* contribute to carrier localization in this case) provides one possible explanation for this observation.

The European Research Council has provided financial support under the European Community's Seventh Framework Programme (FP7/2007-2013)/ERC grant agreement no 279361 (MACONS). This work was also funded in part by the EPSRC (Grant Nos. EP/H047816/1, EP/H0495331 and EP/J003603/1).

[1] T. Mukai, M. Yamada, and S. Nakamura, Jpn. J. Appl. Phys. **38** (7R), 3976 (1999).
[2] S. Nakamura, Science **281** (5379), 956 (1998).
[3] J. Speck and S. Chichibu, MRS Bull. **34** (05), 304 (2009).
[4] S. F. Chichibu, A. Uedono, T. Onuma, B. A. Haskell, A. Chakraborty, T. Koyama, P. T. Fini, S. Keller, S. P. Denbaars, and J. S. Speck, Nat. Mater. **5** (10), 810 (2006).
[5] T. Sugahara, H. Sato, M. Hao, Y. Naoi, S. Kurai, S. Tottori, K. Yamashita, K. Nishino, L. T. Romano, and S. Sakai, Jpn. J. Appl. Phys. **37** (4A), L398 (1998).
[6] D. Graham, A. Soltani-Vala, P. Dawson, M. Godfrey, T. Smeeton, J. Barnard, M. Kappers, C. Humphreys, and E. Thrush, J. Appl. Phys. **97** (10), 103508 (2005).
[7] R. Oliver, S. Bennett, T. Zhu, D. Beesley, M. Kappers, D. Saxey, A. Cerezo, and C. Humphreys, J. Phys. D: Appl. Phys. **43** (35), 354003 (2010).
[8] M. J. Galtrey, R. A. Oliver, M. J. Kappers, C. J. Humphreys, D. J. Stokes, P. H. Clifton, and A. Cerezo, Appl. Phys. Lett. **90** (6), 061903 (2007).
[9] M. Galtrey, R. Oliver, M. Kappers, C. Humphreys, P. Clifton, A. Cerezo, and G. Smith, Appl. Phys. Lett. **91** (17), 6102 (2007).
[10] C. Kisielowski and T. Bartel, Appl. Phys. Lett. **91** (17), 176101 (2007).
[11] D. Gerthsen, E. Hahn, B. Neubauer, A. Rosenauer, O. Schön, M. Heuken, and A. Rizzi, Phys. Status Solidi A **177** (1), 145 (2000).
[12] T. Smeeton, M. Kappers, J. Barnard, M. Vickers, and C. Humphreys, Appl. Phys. Lett. **83** (26), 5419 (2003).
[13] K. H. Baloch, A. C. Johnston-Peck, K. Kisslinger, E. A. Stach, and S. Gradečak, Appl. Phys. Lett. **102** (19), 191910 (2013).
[14] S. E. Bennett, T. M. Smeeton, D. W. Saxey, G. D. Smith, S. E. Hooper, J. Heffernan, C. J. Humphreys, and R. A. Oliver, J. Appl. Phys. **111** (5), 053508 (2012).
[15] J. R. Riley, T. Detchprohm, C. Wetzel, and L. J. Lauhon, Appl. Phys. Lett. **104** (15), 152102 (2014).
[16] T. Prosa, P. Clifton, H. Zhong, A. Tyagi, R. Shivaraman, S. Denbaars, S. Nakamura, and J. Speck, Appl. Phys. Lett. **98** (19), 191903 (2011).
[17] S. E. Bennett, D. W. Saxey, M. J. Kappers, J. S. Barnard, C. J. Humphreys, G. D. Smith, and R. A. Oliver, Appl. Phys. Lett. **99** (2), 021906 (2011).
[18] M. Takeguchi, M. Mccartney, and D. J. Smith, Appl. Phys. Lett. **84** (12), 2103 (2004).
[19] M. P. Moody, L. T. Stephenson, A. V. Ceguerra, and S. P. Ringer, Microsc. Res. Tech. **71** (7), 542 (2008).
[20] L. T. Stephenson, M. P. Moody, P. V. Liddicoat, and S. P. Ringer, Microsc. Microanal. **13** (06), 448 (2007).

[21] C. Johnston, M. Kappers, M. Moram, J. Hollander, and C. Humphreys, J. Cryst. Growth **311** (12), 3295 (2009).
[22] R. Oliver, F.-P. Massabuau, M. Kappers, W. Phillips, E. Thrush, C. Tartan, W. Blenkhorn, T. Badcock, P. Dawson, and M. Hopkins, Appl. Phys. Lett. **103** (14), 141114 (2013).
[23] M. Vickers, M. Kappers, T. Smeeton, E. Thrush, J. Barnard, and C. Humphreys, J. Appl. Phys. **94** (3), 1565 (2003).
[24] F.-P. Massabuau, S.-L. Sahonta, L. Trinh-Xuan, S. Rhode, T. Puchtler, M. Kappers, C. Humphreys, and R. Oliver, Appl. Phys. Lett. **101** (21), 212107 (2012).
[25] T. Zhu, C. F. Johnston, M. J. Kappers, and R. A. Oliver, J. Appl. Phys. **108** (8), 083521 (2010).
[26] F. Tang, M. P. Moody, T. L. Martin, P. A. Bagot, M. J. Kappers, and R. A. Oliver, "Practical issues for atom probe tomography analysis of III-nitride semiconductor materials," Microsc. Microanal. **Under review** (2014).

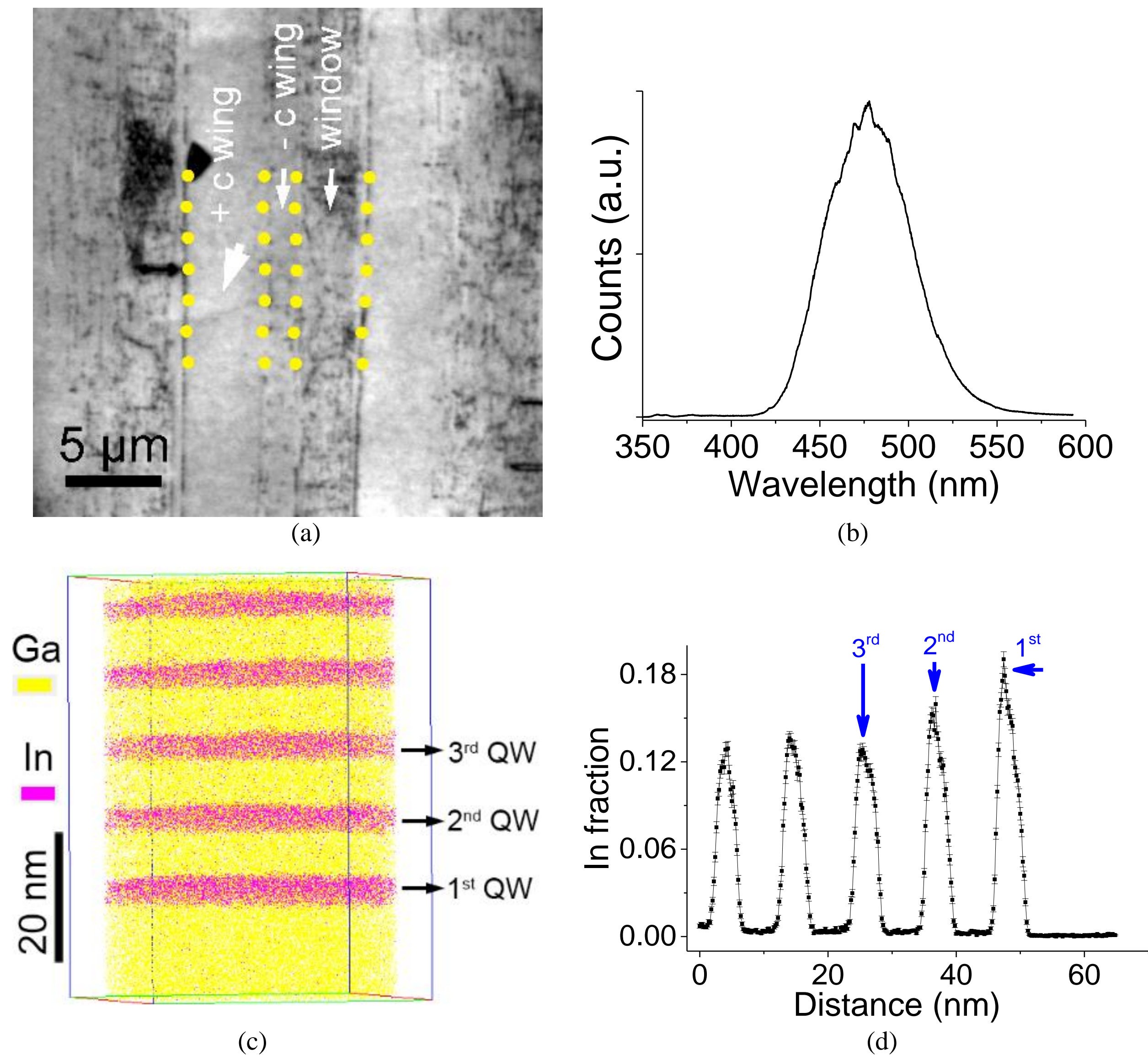

FIG. 1 SEM-CL and APT analysis of the *a*-plane InGaN/GaN QW structure. (a) A panchromatic CL image, in which the large arrow points out the central regions for extracting APT samples; (b) the corresponding CL spectrum; (c) a 3D APT reconstruction (grid box of 45 × 45 × 65 nm) showing the reconstructed 80% In and 10% Ga atoms for clarity and (d) the corresponding 1D concentration profile of In fraction.

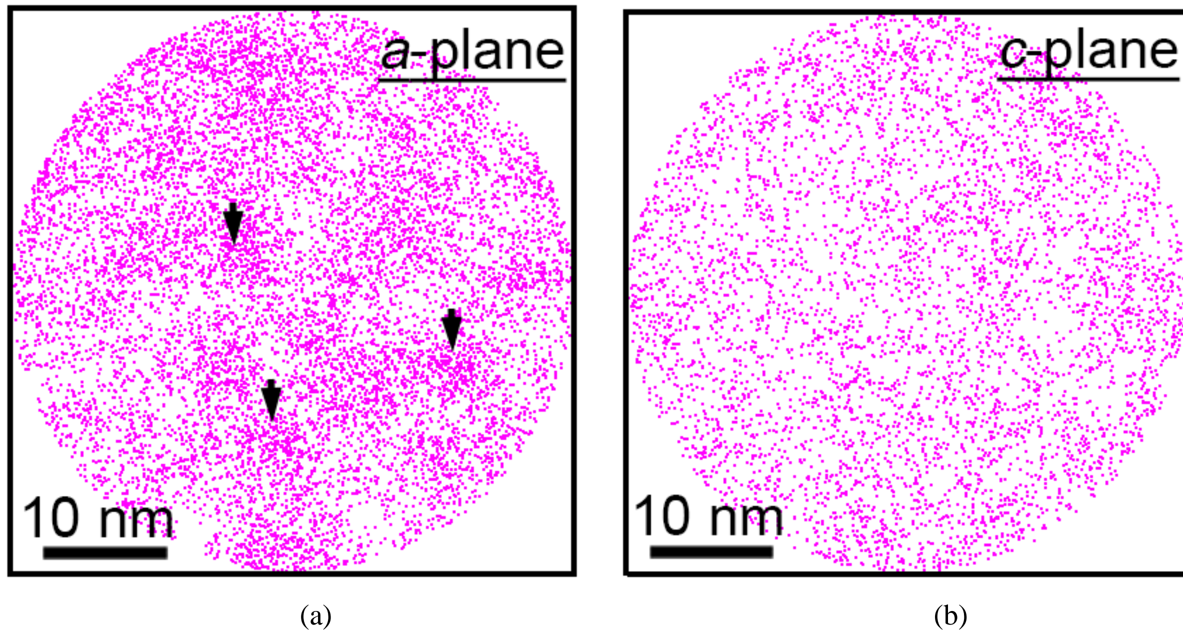

(a) (b)

FIG. 2 Colour map of In atoms projected on the X/Y plane of the 2nd QWs from the *a*-plane (a) and *c*-plane (b) samples. The volumes were extracted using interfaces at the half maximum of In contents, i.e., In fractions of 0.075 and 0.082 for the *a*- and *c*-plane samples respectively. In (a) the arrows point out some 'blotchy' areas associated with locally increased In atoms.

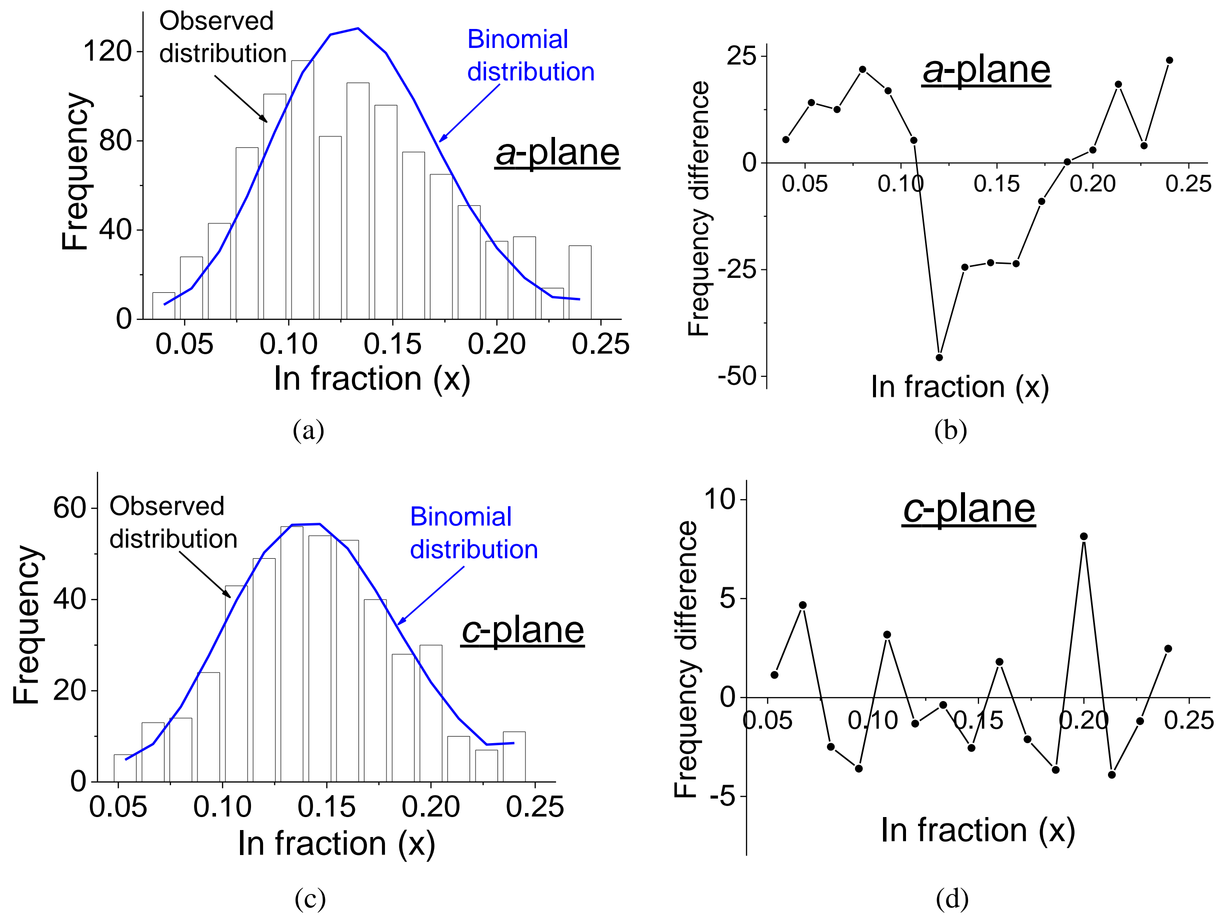

FIG. 3 A representative FD analysis of the 2nd QWs from both *a*-plane ((a) and (b)) and *c*-plane ((c) and (d)) samples using the 75-atom bin size. A $\chi 2$ statistic shows a p-value less than < 0.001 in (a) and a p-value 0.78 in (c) respectively.

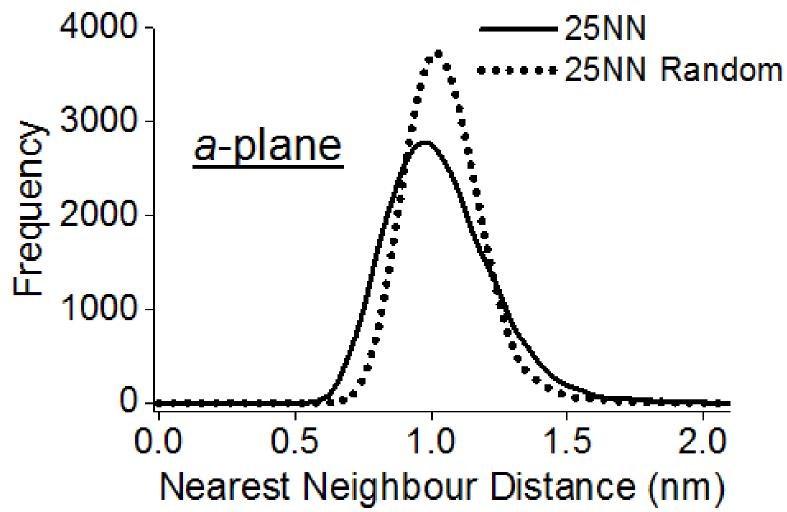

(a)

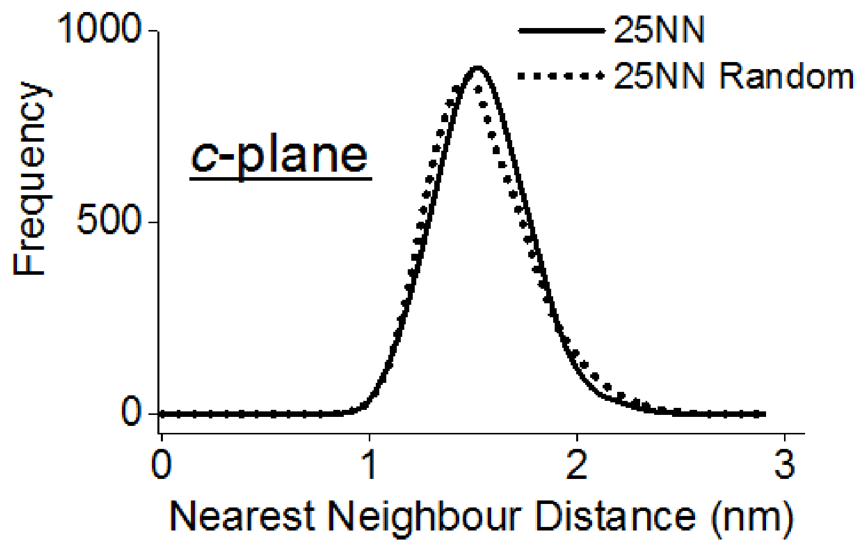

(b)

FIG. 4 Modified NN analysis of the 2nd QWs from *a*-plane (a) and *c*-plane (b) samples showing the 25NN case. The result indicates a strong statistical evidence of significant clustering of In atoms in *a*-plane QW, but not in *c*-plane, when comparing with their corresponding random distributions.